International Journal of Environmental Sciences
ISSN: 2229-7359
Vol. 11 No. 23s, 2025
https://www.theaspd.com/ijes.php

Optimized Reconfiguration Of PV Arrays Under Partial Shading Using The Snake Algorithm

Ghusoon A. Aboud[a], Maher T. Alshamkhani[b], Masad Mezher Hasan[c,b,*], Ahmed Khaldoon Abdalameer[d]

[a]Department of Engineering Affairs, University of Fallujah, Iraq.
[b]Department of Fuel and Energy, Basra Engineering Technical College, Southern Technical University, Basra, Iraq
[c] School of Chemical Engineering, Universiti Sains Malaysia, 14300, Nibong Tebal, Penang, Malaysia.
[d] School of Electrical & Electronic Engineering, Engineering Campus, Universiti Sains Malaysia, 14300 Nibong Tebal, Penang, Malaysia.
[*]Corresponding Author: ghusoon.ajieb@uofallujah.edu.iq Ghusoon A. Aboud

Abstract

The performance of photovoltaic (PV) systems is significantly diminished under partial shading due to uneven sunlight exposure, leading to considerable energy losses. While many fixed and adaptive reconfiguration methods have been investigated, environmental factors such as irregular sunlight, snow, frost, and dust further complicate optimal energy harvesting. This research introduces an innovative reconfiguration strategy that utilizes the Snake Optimizer (SO) algorithm to improve PV array performance under partial shading conditions. The proposed SO-based method specifically aims to minimize current imbalances across array rows while maximizing overall power output. The four shading scenarios were short wide (SW), long wide (LW), short narrow (SN), and long narrow (LN).Through MATLAB-Simulink simulations of the proposed method, several standard algorithms including: Total Cross Tied (TCT), Butterfly Optimization Algorithm (BOA), Harris Hawks Optimization (HHO) and Flower Pollination Algorithm (FPA) were compared also show the proposed algorithm to be effective.PV power output had significant increases: 37.5% shorter wide, 22.7% long wide, 19.7% shorter narrow and 12.9% long narrow.Without a doubt these results offer insight into the potential of the SO algorithm to provide an efficient and reliable way for increasing PV energy harvests in real-world environments where shading occurs.

Keywords: Dynamic array reconfiguration, Enhancing power generation, Solar photovoltaic (SPV), Partial shading in PV systems, Snake optimizer.

1. INTRODUCTION

Thanks to the global proliferation of environmentally friendly trains, renewable energy has replaced fossil fuels. Meanwhile, the photovoltaic panels installed in solar-powered engines transform solar radiation into electric energy much more effectively. But a large part of this progress is due to the increasing efficiency of photovoltaic cells, which is strongly influenced by both solar irradiance and ambient temperature（Petrychenko et al.,2025; Rumbayan et al.,2025）. The global maximum power (GMP) represents the optimal operating point on the voltage-power curve under full sunlight conditions. However, the Partial Shading Conditions (PSCs) lead to voltage fluctuations and reduced power output, which seriously hamper PV systems. In PSCs, the voltage-power curve exhibits plenty of local maxima besides GMP; this further complicates power optimization. Many factors lead to shading of the solar array, including dust, buildings, foliage, poles and clouds. Yet, though using bypass diodes in parallel PV panel arrangements can indeed mitigate the effects of shading, it also can introduce mismatch losses and create multiple peaks in the power curve（Baka et al.,2019; Oko et al.,2012）.

Reconfiguring the PV array has become a popular method for overcoming these problems. It is believed that reconfiguration will cut back on shading effects and boost power extraction (Hasan and Genç, 2022; Pillai et al., 2018; Romli et al., 2016). This is a critical technique for keeping PV systems running at peak efficiency. As shading conditions change, it adapts to them. (Hasan et al., 2023; Kumar and Rao, 2016; Mao et al., 2020). Reconfiguration methods for a PV array can be divided in two: static and dynamic methods (Rezk et al., 2021; Romli et al., 2016; Talukdar, 2017). With static methods. PV modules are physically relocated to minimize shading effects (Handayani and Ariyanti, 2012; Hasan et al., 2022; Malathy and Ramaprabha, 2018), while dynamic methods change the electrical connections between modules so that they can quickly adapt to new shading patterns (Dellosa, 2016; Jabbar et al., 2023; Mohammad et al., 2023; B. Yang et al., 2021); Both methods are essential for improving the efficiency and reliability of PV arrays in actual operating conditions where sunlight exposure is not uniform. Different configurations such as: SP (single level sub-string configuration), TCT (total current transfer), BL (block level) and HC (hybrid configuration) were taken under study for the performance of these modules. (Mao et al., 2020) However, despite all this work, the challenge of motling is hardly begun yet. For example, Youni (Rezk et al., 2021) employed the hill climbing technique to transform PV arrays into geometric configurations with less shading, in order that its power generation may be boosted anew. Recent research also includes comprehensive examinations of strategies to reconfigure (Malathy and Ramaprabha, 2018) and increase (Yang et al., 2021) power generation from PV arrays. One paper introduced the/building-skyscraper-method to resolve shading effects (Anjum and Mukherjee, 2022), while another discussed how to crystallize into something fair energy harvests under shade conditions, particularly getting the GMP out (Aljafari et al., 2022). Moreover, the Grasshopper Optimizer technique (Fathy, 2018) was utilized to enhance power generation, while Ant Colony Solution (ACS) algorithm was developed in (Cao et al., 2020) to allow PV modules to find their optimal locations and excel beyond traditional TCT settings. Other notable methods include, the Ken-Ken puzzle module (Palpandian et al., 2021), Genetic Algorithms (GA) (Matha and Rao, 2020), and Sudoku-based arraying (Krishna and Moger, 2018). Similarly, the Innovative Capability Square approach (Kumar and Raushan 2024) and also Secondary Lo Shu strategy (Venkateswari and Rajasekar, 2021)were both tested for reconfiguring PV elements. A new strategy Recursive Addition was proposed to prevent PV modules of the same row from being adjacent (Yadav et al., 2023).

In order to improve PV systems, many advanced meta-heuristic algorithms advanced by scholars are done by researchers. A novel technique introduced by Yadav et al.(2023) for PV array reconfiguration optimization is Vommi. Particle Swarm Optimization (PSO) was used to eliminate the influence of shadows and increase power generation.(Youlksi et aL.2020b) Harris Hawks Optimizer (HHO) (Yousri et al., 2020a) was applied in the best configuration of the switching matrix. But it is still limited to exploring in complex scenarios. Also, other notable algorithms such as the Honey Badger Algorithm (HBA) (Hans et al., 2023) and Artificial Bee Colony (ABC) (Huynh et al 2023), the former has yet proved unsatisfactory for practical application in this area due to low convergence speed coupled with local optima sensitivity problems; whereas the latter is extremely complicated and involves long computing processes.

There are three widely used algorithms currently: Butterfly Optimization Algorithm (BOA), Harris Hawks Optimization (HHO) and Flower pollination algorithm Factoring the array by welding joints could increase output heterogeneously--but each has its own disadvantages.BOA (Kroll et al., 2018)In general, these methods have drawbacks.

Their convergence is slow, sometimes they fall into local optimums, and computational complexity is higher which is not conducive to actual real-time applications. (Fathy, 2018; Youlksi et al., 2020a)

In his latest paper on 22 May 2022 Alzahwi and et kc's fifteen characteristics of snakes were portrayed in a set phrases with high biological meanings; for this had been a brand-new kind bio-algorithm that on somewhat of ist own devloped from natural reproduction survival conducts as well - doing well too--for its productivity at fast ment he period between certain steps for solute reactions is determined more so by physics power -. The snake optimization algorithm (and) of these unique adaptive links, received weight analysis from the authors not only of ian this and other Mainland papers but let the contribution of Dong Wang summaries via social medias even though they are going off hard as a tangent in exactly what meaning can most people hope to find. Rolling back to the 2011 epoch we find that publication of Goncalves and et al's fifteen characteristics of snake behavior, first advocates the unique phase transitional links derived from snake reproductive system and survival encounters. Compared with earlier methods, the Snake Optimizer drastically lowers danger of stalling whilst dynamically balancing between global and local searches. This makes it particularly suitable for complex optimization problems, earlier examples of which are to be found.

These theoretical advantages translate into important benefits for the actual operation of a PV array. It enables optimizations in such a way as to quickly and reliably adjust to the changing environmental conditions. Because the snake method can find a quick and robust solution without added convergence process, it must be chosen in this research on grounds of enhanced robustness,faster convergence and higher overall performance than traditional optimization methods.

This work's pivotal contributions to optimizing PV systems are outlined as follows:

• PV Reconfiguration Method Advances: To deal with the influence of partial shading and they resort to a Snake Optimizer algorithm with Stocking technique.

• Detail Shading Analysis: We make an in-depth study on four different shading patterns (m SW, LW, LN and SN) and their respective effects on the performance of the PV array.

• Simulation in Matlab-Simulink has been applied so as to prove the superiority of the SO method by contrast with traditional methods like TCT, BOA, HHO, FPA.

• Improved Power Distribution & Rebalance: By regulating the current balance in each row of the PV array, this method turns out favoring additional electricity generation ways.

• Performance Comparison: Through extensive comparative testing, the SO emerges as highly effective in a variety of partial shading situations when gauge

• Fuel savings in thermo photo-voltaic are strongest, followed by traction energy replacement. Wind turbine yield typically comes last.

• On office network, bandwidth statistics work will begin after an IT infrastructure plan is approved for computer control.

• Key performance indicators such as FF, ML, efficiency, power gain ETC are thoroughly compared to evaluate the algorithm.

The remainder of this paper is structured as follows: Section 2 presents the PV equivalent circuit model; Section 3 explains the TCT configuration; Section 4 introduces the Snake Optimizer (SO) algorithm and its key features; Section 5 details the proposed SO approach PV array; Section 6 discusses the simulation results and evaluates the SO-based PV reconfiguration under different shading patterns; Section 7 Assessment Criteria for PV Array Performance; and Section 8 concludes the study with key findings.

2. MODELING OF PV MODULE

The performance of a photovoltaic system heavily depends on its module quality, composed of several linked solar cells. Due to their non-linear characteristics, researchers have focused extensively on modeling PV cells (Mahdavi et al., 2025). To optimize power generation, three major diode-based models namely, the single-diode (SD) model (Yousri et al., 2019a), the two-diode (DD) model (Pandey and Sandhu, 2014), and the three-diode (TD) model (Mirjalili et al., 2016) have been formulated to enhance power output. For simplicity, fewer parameters, and for reality of installation (Mirjalili et al. 2016; Yousri et al., 2019b), the SD model is the most popular.However, the SD model is selected in this study for PV array implementation because of its simplicity and the fact that it is widely used in real PV applications.The graphical representation of the SD model, appears in Mirjalili et al. (2016), is Figure 1.

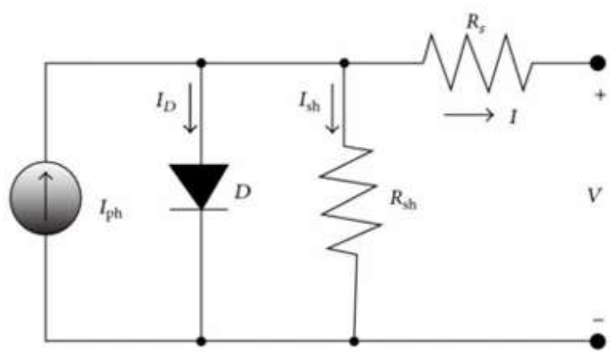

Figure 1 shows the single diode PV model electrical circuit diagram (Mirjalili et al., 2016).

The current-voltage (I-V) characteristics of the SD model can be expressed in Equation (1) (Mirjalili et al., 2016):

$$\boldsymbol{I = I_{ph} - I_0\left(exp\left(\frac{q(V+IR_s)}{\alpha KT}\right) - 1\right) - \frac{V+IR_s}{R_{sh}}} \quad (1)$$

The total current (I) generated by the PV panel depends on several main parameters. is defined as the photocurrent generated by the panel and is its diode leakage current. Panel voltage is indicated by the symbol V, while Rs and are series and shunt resistances respectively for this circuit. Also, q refers to the charge of an electron and K is Boltzmann's constant - α is a description factor applying to the behavior of diodes within PV systems.

3. TCT CONFIGURED PV ARRAY

Inside a photovoltaic module, there are multiple solar cells. A PV array consists of several PV modules connected together. A TCT configuration involves joining PV modules in parallel by rows. The rows are then linked in series. This type of configuration is usually illustrated in Figure (2) (Cao et al., 2020). For this research, a 9×9 TCT grid was employed: this contains 81 PV modules, with each module consisting of nine rows and nine columns. A specific number is assigned to each module in the array so that it can be recognized.

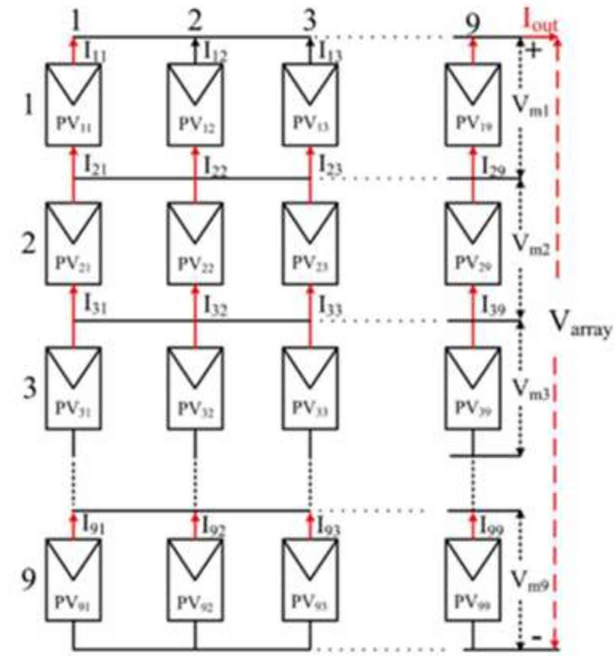

In figure 2, PV modules for each 9×9 square use the Total Cross-Tied (TCT) layout [10].

The character system number the first number of Fig. 2 (i) represents a whitehr this module belongs to, second number (j) shows its level. Module 75, for example, is in the 7th row and 5th column of the area. In this way, the system provides correct representation of what each module 's current will be. The electric output current from modules label Iij may be defined by such an equation:

$$I_{ij} = K_{ij} \times I_m \quad (2)$$

is the current of a PV module under standard irradiance (G = 1000 W/m²), where besides Kij as before is the ratio of the irradiance unit area received by module ij, Gij to the standard irradiance Go.

Expressing the features of solar cell I/V curves, most manufacturers provide values for their products that have been measured under standard conditions, i.e. 25 C and go = 1000 W/m2.

Using Kirchhoff s Voltage Law (KVL), the total voltage V of the array is given byas Equation (3):

$$V_a = \sum_{i=1}^{9} V_{mi} \quad (3)$$

where is the total voltage of the PV array, stands for the voltage of i-th column.

The total current of each row is calculated similarly in Equation(4) as follows:

$$I_{ai} = \sum_{i=1}^{9} I_{mi} \quad (4)$$

where is the sum of all current flowing through the ith row of the PV array.Analysis using this mathematical framework as basis helps us research the distribution of power and optimize PV arrays under partial shading conditions (PSCs).Based on this architecture, the reconfiguration techniques proposed in this paper, which are SO-based, enhance power extraction and seek to equalize current for each branch of the array.

4. SNAKE OPTIMIZATION ALGORITHM METHODOLOGY

Hashim and Hussien(2022) A recent bio-inspired metaheuristic algorithm called the Snake Optimizer (SO) was suggested after snake reproductive behavior. Snake mating behavior depends on various environmental factors, such as access to food and temperature. Performing in different phases is how the Snake Optimizer (SO) algorithm takes on the challenge of exerting RGB (red, green, blue) diversity in PV [photovoltaic] arrays. When photovoltaic panels are shaded, some of the modifications in output power-voltage characteristics are not what you expect, yet others may be. You will be exposed to such a complex and puzzling set. The SO algorithm does a good job handling this during its exploration phase. It launches a broad and randomized search across the range of solutions involved, thus reducing danger of falling prematurely into a local minimum Each electroluminescent (EL) image shows that it starts when a certain number of its nodes visible on the boundary are not luminous or the current approaches zero. In contrast, the exploitation phase focuses on quickly improving candidate solutions in hopeful areas, allowing the algorithm accurately to pick out among the various potential solutions the global maximum power point as one might call this among many synonyms or equivalent phrases. These two phases work together. They are directed by environmental cues like temperature or the availability of resources, enabling the SO algorithm to succeed in a balanced way that changes with new conditions as they arise. Being adaptable is key to optimizing PV systems that have both substantial oscillations and points of local optima. The SO algorithm has two stages engaged in primarily: exploration and also innovation. In the earlier phase, snakes roam about looking for food in order to fill their stomachs when it's cold and there are few available resources. By simulating a broad optimization search, this phase allows the algorithm to explore wider solution spaces and escape from local optima. The exploitation phase starts when it gets hot and food is present. In this phase, snakes converge on promising resources. When food and cold weather coexist, commencement of the mating process takes Snakes display two types of behavior related to mating: competition (this is known as fight mode) and copulation (this is called mating mode). In the first type of behaviour, which is seen 3a where there are male snakes fighting to mate with the fittest female, as well as females trying to choose a good mate for themselves, as in 3b. The second type, copulation, results in pairs of snakes reproducing – depending on food availability as seen in 3b. During mating, there is a chance for eggs to be laid by the female, representing generation of new candidate solutions. By integrating these biological principles, the SO algorithm effectively balances exploration and exploitation, enabling it to navigate complex optimization landscapes efficiently and improve the quality of solutions.

- Snakes in fighting behavior.

a) Snakes in mating behavior.

Figure 3: Illustrative behaviors of snakes during optimization phases.

4.1. Initialization

Like other metaheuristic algorithms, the SO algorithm begins by randomly generating an initial population using a uniform distribution to commence the optimization process. The positions of the individuals in the initial population are determined using the following equation:

$$X_i = X_{min} + r \times (X_{max} - X_{min}) \quad (5)$$

where X_i represents the position of the i_{th} individual in the population, r is a random value ranging between 0 and 1, X_{min} and X_{max} define the lower and upper bounds of the optimization problem, respectively. This initial random setup promotes diversity, allowing the SO algorithm to broadly navigate the solution domain.

4.2. Dividing the swarm into two equal groups males and females

In this study, it is assumed that the population consists of an equal number of males and females, with a 50-50 distribution. To organize the population, the population is divide into two distinct groups: a male group and a female group. This gender-based split is defined using specific mathematical expressions as follows:

$$N_m \approx \frac{N}{2} \quad (6)$$

$$N_f = N - N_m \quad (7)$$

N, as sprinkled at the end of other points, stands for the total number of individuals in the population, Nm means the number of male individuals, and Nf is the number of female individuals. This gender-based community should be recognized as a balanced structure and is essential for the success of the SO algorithm.

4.3. Evaluate each group & defining temperature and food quantity

The process is to choose top performers from the venues in different bodies, and to find the most favorable food item which are represented as fbest,m x and fbest,f y with ffood.

$$Temp = exp(\frac{-t}{T}) \quad (8)$$

The temperature T (!) parameter represents the number of iterations that are allowed before a divergence is reported. An evaluation is made as to how much food the snake is able to find (i.e.()) ~ this has an effect on its behavior at any given time:

$$Q = c_1 \times exp\ (\frac{t-T}{T}) \quad (9)$$

where is a constant which is set to 0.5. This mathematical framework is vital to the snake optimizer algorithm, maintaining an appropriate balance during optimization between exploration and exploitation

4.3.1. Exploration phase (no food)

While the snakes are using up food there is nothing productive until the end of a generation. Below a level of 0.25, snakes pump randomly across solution space. This section of the algorithm uses a mathematical approach to mimic exploration behavior.

$$X_{i,m}(t+1) = X_{rand,m}(t) \pm c_2 \times A_m \times \left((X_{max} - X_{min}) \times rand + X_{min}\right) \quad (10)$$

where $X_{i,m}$ represents the position of the i_{th} male snake, $X_{rand,m}$ is the position of a randomly selected male snake rand is a random number in the range [0, 1] and the diversity factor (±) ensures dynamic adjustments in position, promoting better exploration of the search space. This operator introduces random motion to prevent the algorithm from settling early on suboptimal solutions. The approach is inspired by concepts used in Hunger Games Search (HGS) (Yang et al., 2021), where similar equations are randomly swapped to enhance optimization efficiency. The A_m signifies the male snake's ability to find food, calculated as:

$$A_m = exp\left(\frac{-f_{rand,m}}{f_{i,m}}\right) \quad (11)$$

where $f_{rand,m}$ denotes the fitness of the randomly selected male snake $X_{rand,m}$. The $f_{i,m}$ represents the fitness of the i_{th} male snake. Similarly, for female snakes, their position is updated using the following equation:

$$X_{i,f} = X_{rand,f}(t+1) \pm c_2 \times A_f \times ((X_{max} - X_{min}) \times rand + X_{min}) \quad (12)$$

where $X_{i,f}$ denotes the position of the i_{th} female snake, $X_{rand,f}$ is the position of a randomly selected female snake, rand again is a random number between 0 and 1. The constant c_2 has a value of 0.05. The A_f represents the female snake's ability to find food, calculated as:

$$A_f = exp\ exp\ \left(\frac{-f_{rand,f}}{f_{i,f}}\right) \quad (13)$$

where $f_{rand,f}$ represents the fitness of $X_{rand,f}$, and $f_{i,f}$ is the fitness of the i_{th} female snake.

By implementing these equations, the SO algorithm effectively balances exploration, allowing snakes to search for optimal positions within the solution space. This method enhances the optimizer's ability to navigate complex landscapes and avoid early convergence to local optima.

4.3.2. Exploitation Phase (When Food is Available)

In the exploitation stage, snakes change their position in response to environmental cues like heat and available nourishment. The decision-making process depends on these conditions. The conditions are If (Q) > Threshold, and when the temperature exceeds a certain level, snakes head straight for the food source using the following equation:

$$X_{i,j}(t+1) = X_{food} \pm c_3 \times Temp \times rand \times \left(X_{food} - X_{i,j}(t)\right) \quad (14)$$

where $X_{i,j}$ represents the position of an individual snake (male or female), X_{food} denotes the location of the best-performing individuals, and c_3 is a constant with a value of 2. In cooler setting (i.e. below 0.6), snakes alternate between competitive and reproductive behaviors.

In the Fight Mode (Competition Among Snakes), male snake positions are adjusted based on their behavior during this phase, as follows:

$$X_{i,m}(t+1) = X_{i,m}(t) + c_3 \times FM \times rand \times \left(Q \times X_{best,f} - X_{i,m}(t)\right) \quad (15)$$

where $X_{i,m}$ is the position of the i_{th} male, $X_{best,f}$ represents the best-positioned female, FM denotes how capable the male is in competition scenarios, which is defined as follow:

$$FM = exp\left(\frac{-f_{best,f}}{f_i}\right) \quad (16)$$

where $f_{best,f}$ is the fitness of the top-performing female, and f_i is the fitness of the current individual. On the other hand, female positions are recalculated using a separate update rule, as follow:

$$X_{i,f}(t+1) = X_{i,f}(t+1) + C_3 \times FF \times rand \times \left(Q \times X_{best,m} - X_{i,F}(t+1)\right) \quad (17)$$

where $X_{i,f}$ is the position of the i_{th} female, $X_{best,m}$ represents the top-performing male and the FF indicates the combat strength of the female participant, which is defined as:

$$FF = exp\left(\frac{-f_{best,m}}{f_i}\right) \quad (18)$$

where $f_{best,m}$ is the best fitness score among males.

In contracts in the Mating Mode (Reproduction and Offspring Generation), male and female snakes reposition themselves in coordination with one another. The male's position is updating as a part of the mating process which calculated as follow:

$$X_{i,m}(t+1) = X_{i,m}(t) + c_3 \times M_m \times rand \times \left(Q \times X_{i,f}(t) - X_{i,m}(t)\right) \quad (19)$$

Similarly, the female's position is updating based on mating behavior as follow:

$$X_{i,f}(t+1) = X_{i,f}(t) + c_3 \times M_f \times rand \times \left(Q \times X_{i,m}(t) - X_{i,f}(t)\right) \quad (20)$$

where M_m and M_f represent mating strength for both genders is computed through specific equations:

$$M_m = exp\left(\frac{-f_{i,f}}{f_{i,f}}\right) \quad (21)$$

$$M_f = exp\left(\frac{-f_{i,m}}{f_{i,f}}\right) \quad (22)$$

where $f_{i,f}$ and $f_{i,m}$ are the fitness scores of individual females and males.

4.5. Offspring Selection and Population Update

When offspring are generated, the least fit male and female candidates are replaced:

$$X_{worst,m} = X_{min} + rand \times (X_{max} - X_{min}) \quad (23)$$

$$X_{worst,f} = X_{min} + rand \times (X_{max} - X_{min}) \quad (24)$$

where $X_{worst,m}$ and $X_{worst,f}$ are the least fit male and female individuals, respectively.

4.6. Termination Criteria

The Snake Optimizer runs iteratively until a set stopping rule is triggered. If the convergence condition is satisfied, the process terminates, ensuring that an optimal solution is found.

5. METHODOLOGY

The preconditions will be satisfied, which will cause PV arrays under shadow to per-form is better than ever thanks an optimization framework based on snake algorithm. The hunting, competition and reproduction behaviors among snakes were the biological inspiration behind this algorithm. The algorithm can flexibly adjust its strategy as they range from broad exploration to optimization. Each member of the population, this approach represents a possible arrangement for PV modules - e.g., on a total cross tied layout. Simultaneously we evaluate the overall fitness in order to maximize the total power output and minimize current mismatch across array. In the next subsections, we will explain how to implement the Snake Optimization Algorithm for PV arrays.

5.1. Candidate Initialization

The process of optimisation begins by randomly creating candidate solutions. Each candidate solution, denoted as Y, respectively defines a potential configuration of the modules of PV. The initial position of each candidate is determined from equation (25):

$$X_i = X_{min} + r \times (X_{max} - X_{min}) \qquad (25)$$

where i is a uniformly distributed random number beginning between 0 and 1, and W represent the lower and upper boundaries of the design space directions respectively. This random initialization promotes a broad starting point for searches and helps tap into the worldwide good results.

5.2. Population Division

In order to mimic the natural mating mode for snakes, all the creatures in the population are split into two equal parts: women and men.By splitting domestic labor from industrial production mathematically in (6) and (7), this system has succeeded in playing for a long time different dynamics of behavior during subsequent optimization steps.While mixed-gender populations may sometimes result in competitive friction between the sexes (fight mode) and at other times cooperative relations between them (mating mode).Rebalancing the sex ratios is crucial because it creates an environment that is conducive to fighting as well as mating.

5.3. Fitness Evaluation and Environmental Parameters

5.3.1 In a composite fitness function, every candidate solution has to be assessed by combining two important objectives:

5.3.2 Power Maximization:

Objective This aims to maximize the total delivered power by adding Ix? Vx over the number of PV rows then multiplying it by.

5.3.3 Current Mismatch Minimization:

This requires minimizing the current matching, i. | Imax - I' | o ensure a uniform current distribution across array.

These two objectives are balanced within one single composite function through a tunable parameter,, as shown in Equation (26):

$$f(X_i) = -\left(\sum_{x=1}^{9} \quad (I_x \times V_x)\right) + \lambda \, . |I_{max} - I_{min}| \qquad (26)$$

where is a weighting factor that contrasts the importance of two different objectives with weights. Meanwhile, the algorithm also calculates two new environmental parameters which change dynamically:

a balanced gender distribution is essential, allowing for both competition (the fight mode) and cooperation (the tie-up mode).

a) Temperature (Temp): Defined by Equation (8), this parameter decreases~multiplying itself each time it does so~exponentially with iteration count to make Exploration the initial phase in an algorithm [step through settling down]. b) Food Quantity (): As calculated in Equation (9), this quantity operates through an activation threshold comparison to direct the exploration or exploitation model.

5.4. Exploration Phase

As the amount of food computed drops below a predefined threshold (0.25 in this study), the algorithm starts an exploration phase: In this phase, candidates move their positions by a random walk over the solution space. The motion of male and female candidates is a function of Equations (10) and (12), respectively. In the exploration phase, a dynamic operator known as the±diversity factor urges candidates to randomly change their current positions. This in turn helps prevent premature convergence to local optima. The ability of any candidate to find a better place is influenced by the performance factorsAmcf, which are calculated by Equations (11) and (13) for males and females respectively.

5.5. Exploitation Phase

As conditions improve (i.e., when $Q > 0.6$), the algorithm transitions into the exploitation phase. The mode of exploitation depends on the current temperature, referred to as Temp:

a) Hot Exploitation (High Temperature):

If Temp > $Temp_{threshold}$, candidates are directed toward the best-known configuration (the food position) using Equation (14).

b) **Cold Exploitation (Low Temperature):**

where Temp ≤ $Temp_{threshold}$, the algorithm exhibits two distinct behaviors. The fighting mode is the first behavior, where male candidates update their positions by moving aggressively toward the best female candidate, while female candidates adjust their positions toward the best male counterpart. This movement is expressed by Equation (15) for males and Equation (17) for females. The fighting abilities FM and FF are calculated using Equations (16) and (18), respectively.

The second behavior is the Mating Mode, where paired candidates (a male and a female) update their positions cooperatively. This mutual adjustment is performed according to Equations (19) and (20). The corresponding mating abilities M_m and M_f are obtained from Equations (21) and (22).

5.6. Offspring Selection and Population Update

To maintain diversity and prevent stagnation, the algorithm replaces the least fit candidates with new, randomly generated solutions. This replacement is carried out using Equations (23) and (24), which reinitialize the worst-performing male and female individuals.

5.7. Termination Criteria

The process of this algorithm continues until it meets a preset stop criterion. That may be when a maximum number T of iterations is called or if the combined change in fitness throughout the population falls below some threshold point in training, depending on conditions at hand. At this stage, the candidate solution with the highest fitness (i.e., maximum total power output and smallest current mismatch) is selected to become optimal PV configuration. SO methods have the potential advantage of adapting a function quickly enough to account for changes while it is still accurate:

As dynamic reconfiguration and adaptability: Influenced by the foraging and mating habits of snakes, the snake optimizer algorithm is responsive to diverse environmental conditions. For example, if the tint of light or radiation strength is altered, it varies its attack methods accordingly. In this way its adaptability is reflected in outcomes at operation, ensuring that the PV configuration keeps up to date all along by continually trying out different systems and eliminating those which are no longer optimal.

As both exploration and exploitation are in equilibrium: In conclusion, the SO algorithm effectively maintains a balance between exploiting well-known promising areas and exploring new solution spaces. For this balance is essential to PV systems; with partial shading, you can often find local extremes that are much better than anything else nearby-but if they were really all there is, or any worst is better than better yet as elsewhere awaits even furthe away than where all available roads have been tried without success; should Heaven be so unkind as not to release you from such labyrinthian predicament? Balanced Exploration and Exploitation by Wang Ganchang at the CACHE conference 1982

For real-time applications, fast convergence: By introducing natural behavioral cues (e.g. the change to quick direction shifts) into the SO algorithm, we can speed up to hit high-quality solutions. This rapid convergence has particular relevance for PV arrays since they must still produce electricity in real-time or near real-time even when the outdoor conditions are changing.

The SO algorithm is versatile enough to accommodate PV systems of different sizes, small-scale installations to large arrays. Its flexibility in this respect makes it a strong candidate for widespread deployment in diverse energy production environments where there are numerous geographic or other differences.

As both cost-effective and reducing dependence on equipment: By arranging the configuration so as to maximize power output and minimize current mismatch in the array, the SO algorithm can contribute to reducing energy losses. Over the course of time this should mean lower system costs overall as well as less need for large numbers of sensors and switching devices: with just a basic structure requiring less maintenance work in total not much left to go wrong either from one year to another. As a result it will be easier to upgrade such a system lightly more smoothly should future innovations come along either more efficient still without causing any extra trouble at all.Keeping hardware costs downKeeping hardware costs downKeeping hardware costs downNo PROJECTCOMMENTARY

Despite its complexity based on nature instead of human science: Despite the complexity of its bioinspiration, the SO algorithm remains relatively easy to implement. The efficiency with which it utilizes natural behaviors also makes it a practical optimization tool, not taking up too many computational resources but robust in practical use so that one can keep worrying more about results than methods as in today's real-world PV applications.

In short, the method proposed here uses SO algorithm to improve the performance of PV arrays while under partial shading conditions. The task initiates with two sets of candidate solutions, male and female. A composite fitness function (see Equation (25)) is employed to balance the two objectives of maximising power output and minimizing current mismatch. While dynamical environmental parameters such as temperature (Equation (8)) and amount of food (Equation (9)) guide the transition from exploration stage to exploitation phase. In the exploration stage, random perturbations (Equations (10) and (12)) are used to explore solution space, while in exploitation phase more focused movements towards better candidates (Equations (14), (15), (17), (19) and (20)) are made. This phase includes competitive fighting and cooperative mating strategies. Solutions unable to survive are periodically removed and replaced (Equations (23) and (24)). This replenishment keeps diversity in the population alive.

Methods: The next Section of this paper reports on the results of a 500-iteration run for the SO algorithm as it was evolved 30 individuals at once. With standardized conditions--namely an incidence of 1000 W/m² and an ambient temperature 25 ℃--such tests simulate well the performance of PV arrays in an environment partly shaded. The SO-based method ensures that PV layouts are more easy to optimize, by always adjusting and perfecting. It likewise enables us to minimize differences in array performance whilst boosting total power output.

Adhering to widely accepted rules from the literature and making do with untold numbers of computational experiments, we cautiously chose simulation parameters. A population size of thirty was chosen because this is a very common number found in the use of meta-heuristic optimization methods and it makes sure that we keep a wide variety of guesses for solutions under control without running into too much trouble (Hashim and Hussien 2022). Five hundred iterations came from the convergence analysis we made before. The point found was this was about as far which provided adequate exploration and exploitation while not creating excessive noise with extraneous calculations. Environmental thresholds, including temperature threshold 0.25 and food quantity threshold 0.6, were adapted from the original study of Snake Optimizer by Hashim and Hussien (2022). This provided a good balance between exploration and exploitation that could be supported by empirical evidence. Taken together, our selections improve the usefulness and reasonableness of our model for real life scenarios of photovoltaic reconfiguration.

6. RESULTS AND DISCUSSION

The proposed method was tested using a 9 × 9 TCT PV array under various Partial shading conditions (PSCs). Firstly, four sets of shade patterns (SW, LW, SN as well as LN) which led to different levels of irradiance were considered to investigate the functioning of such a system. For Kyocera Solar panels, the PV system employ this configuration. With the results of the proposed SO-based method, we compared them to a standard TCT configuration as well as other optimization algorithms, such as Butterfly Algorithm (BOA), Harris hawks swarm optimization (HHO) and Flower Pollen of Wind (FPA). All the simulations were carried out on a laptop with an Intel Core i7 processor (2.7 GHz), 8 GB RAM and MATLAB 2022. These four different partial shading patterns studied in this paper are depicted as following.

CASE 1: Short-Wide Shading Patter

Under Short-Wide (SW) shading: The array is split into four different sub-arrays, each of which receives its own irradiance level. The first sub-array gives or receives solar radiation equivalent to 900 W/m², the second at 600 W/m², the third 400W/m%, and fourth 200 w/The business method it proposed outperformed other optimization techniques in two respects. Accordingly (Fig. 4e shows this pose as well as the cross-tie of Figure 4a maintains a particular neutrality level by introducing a counter external element. Fig. 4a is connected differently from what might have been conventional wisdom and is indeed unique in the world!

$$I_{R1} = k_{11}I_{11} + k_{12}I_{12} + \ldots k_{19}I_{19} \qquad (27)$$

where k_{11} represents the ratio of the solar irradiance level on the panel located in the first row and first column of the array. This level is normalized against the standard test condition (STC) irradiance level of 900 W/m². In the Total Cross-Tied (TCT) configuration, the row currents follow this pattern:

$$I_{R1} = I_{R2} = I_{R3} = I_{R4} = I_{R5} = 9\times0.9\ I_m = 8.1\ I_m \qquad (28a)$$

$$I_{R6} = 5\times0.6\ I_m + 4\times0.9\ I_m = 6.6\ I_m \qquad (28b)$$

$$I_{R7} = I_{R8} = I_{R9} = 3\times0.6\ I_m + 3\times0.4\ I_m + 3\times0.2\ I_m = 3.6\ I_m \qquad (28c)$$

Detailed calculations for row currents and power outputs across each configuration are summarized in Table 3.

The analysis, as shown in Table 3, reveals that TCT delivered the weakest performance, peaking at just 40.5 W in most trials before falling to 39.6 W and 32.4 W. BOA achieved up to 45.0 W but showed inconsistency, ranging from 8.1 W to 45.0 W. FPA improved peak output to 51.3 W with more stable mid-range results between 13.8 W and 47.2 W. HHO performed better, reaching 53.1 W and staying above 25 W in most cases. The proposed SO method outperformed all others, reaching 55.7 W and consistently maintaining outputs above 45.9 W. Compared to TCT, the proposed method achieved 37.5% more power and also surpassed BOA, FPA, and HHO by 23.8%, 8.6%, and 4.9%, respectively. As shown in Figure 5, the proposed SO also delivered the highest global peak power of 18,200.82 W, while TCT lagged with just 15,300.88 W.

(a)

TCT								
11	12	13	14	15	16	17	18	19
21	22	23	24	25	26	27	28	29
31	32	33	34	35	36	37	38	39
41	42	43	44	45	46	47	48	49
51	52	53	54	55	56	57	58	59
61	62	63	64	65	66	67	68	69
71	72	73	74	75	76	77	78	79
81	82	83	84	85	86	87	88	89
91	92	93	94	95	96	97	98	99

(b)

BOA								
11	12	13	14	15	16	17	18	19
21	22	23	24	25	26	27	28	29
31	32	33	34	35	36	37	38	39
41	42	43	44	45	46	47	48	49
51	52	53	54	55	56	57	58	59
61	62	63	64	65	66	67	68	69
71	72	73	74	75	76	77	78	79
81	82	83	84	85	86	87	88	89
91	92	93	94	95	96	97	98	99

(c)

FPA								
11	12	13	14	15	16	17	18	19
21	22	23	24	25	26	27	28	29
31	32	33	34	35	36	37	38	39
41	42	43	44	45	46	47	48	49
51	52	53	54	55	56	57	58	59
61	62	63	64	65	66	67	68	69
71	72	73	74	75	76	77	78	79
81	82	83	84	85	86	87	88	89
91	92	93	94	95	96	97	98	99

(d)

HHO								
11	12	13	14	15	16	17	18	19
21	22	23	24	25	26	27	28	29
31	32	33	34	35	36	37	38	39
41	42	43	44	45	46	47	48	49
51	52	53	54	55	56	57	58	59
61	62	63	64	65	66	67	68	69
71	72	73	74	75	76	77	78	79
81	82	83	84	85	86	87	88	89
91	92	93	94	95	96	97	98	99

(e)

SO								
11	12	13	14	15	16	17	18	19
21	22	23	24	25	26	27	28	29
31	32	33	34	35	36	37	38	39
41	42	43	44	45	46	47	48	49
51	52	53	54	55	56	57	58	59
61	62	63	64	65	66	67	68	69
71	72	73	74	75	76	77	78	79
81	82	83	84	85	86	87	88	89
91	92	93	94	95	96	97	98	99

900 w/m^2 600 w/m^2 400 w/m^2 200 w/m^2

Figure 4: PV array under the Short Wide (SW) shading pattern, as generated using: (a) TCT, (b) BOA, (c) FPA, (d) HHO, and (e) the proposed SO-based method.

Row	I(A)	V(v)	P(W)
TCT			
R_1	8.1	5	40.5
R_2	8.1	5	40.5
R_3	8.1	5	40.5
R_4	8.1	5	40.5
R_5	8.1	5	39.6
R_6	6.6	6	32.4
R_7	3.6	9	32.4
R_8	3.6	9	32.4
R_9	3.6	9	32.4
BOA			
R_1	6.5	5	32.5
R_2	8.1	1	8.1
R_3	6.1	6	36.6
R_4	5.5	8	44.0
R_5	5.0	9	45.0
R_6	6.5	5	32.5
R_7	5.9	7	41.3
R_8	7.1	3	21.3
R_9	7.2	2	14.4
FPA			
R_1	5.7	9	51.3
R_2	9.9	2	13.8
R_3	6.0	6	36.0
R_4	6.8	4	27.2
R_5	5.9	8	47.2
R_6	5.9	8	47.2
R_7	6.4	5	32.0
R_8	6.8	4	27.2
R_9	7.51	1	7.5
HHO			
R_1	6.1	8	48.8
R_2	6.2	7	43.4
R_3	6.3	6	37.8
R_4	6.3	6	37.8
R_5	6.9	2	13.8
R_6	5.9	9	53.1

R_7	6.6	3	19.8
R_8	6.4	4	25.6
R_9	7.2	1	7.2
SO			
R_1	6.3	8	54.9
R_2	6.5	4	26.0
R_3	6.3	8	50.4
R_4	6.3	8	55.7
R_5	6.9	1	6.9
R_6	6.3	8	50.4
R_7	6.3	8	50.4
R_8	6.1	9	45.9
R_9	6.6	3	19.8

Table 3: Global Maximum Power comparison of TCT, BOA, FPA, HHO, and the proposed SO-based configurations under SW shading scenario.

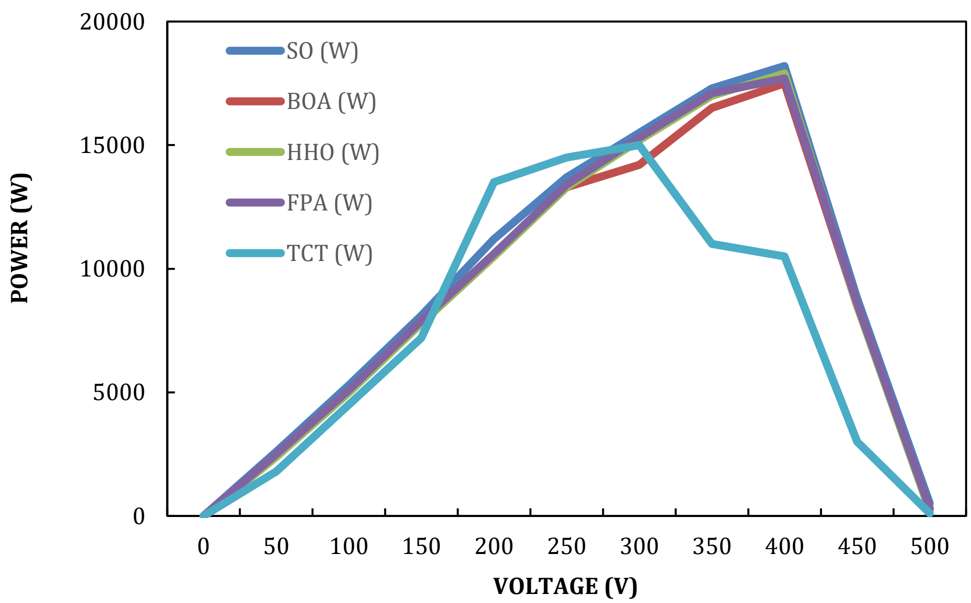

Figure 5: Power-voltage performance of TCT, BOA, HHO, FPA, and SO-based configurations under LW shading scenario.

6.2. CASE 2: LONG WIDE SHADING

Under the LW shading scenario, the PV array receives solar irradiance at five varying levels: 900, 600, 500, 400, and 200 W/m². Figure 6 illustrates the array configurations (TCT, FPA, BOA, and SO), with current calculations shown for TCT in Figure 6a. Rows 7–9 yield 3.6 I_m, while rows 1–6 produce 6.6 I_m, as per Equations (29a) and (29b).

$$I_{R7} = I_{R8} = I_{R9} = 2 \times 0.6\ I_m + 2 \times 0.5\ I_m + 2 \times 0.4\ I_m + 3 \times 0.2\ I_m = 3.6\ I_m \qquad (29a)$$

$$I_{R1} = I_{R2} = I_{R3} = I_{R4} = I_{R5} = I_{R6} = 6 \times 0.9\ I_m + 3 \times 0.4\ I_m = 6.6\ I_m \qquad (29b)$$

Table 4 tabulate detailed performance data. TCT recorded the lowest maximum power (39.6 W), with FPA slightly higher (40.5 W). HHO and BOA reached 46.8 W and 47.7 W, respectively. The proposed SO method delivered the highest output at 48.6 W—22.7% above TCT, 20.0% above FPA, 3.8% above HHO, and 1.9% above BOA.

As shown in Figure 7, TCT had the weakest GMP at 15,001 W, while the SO method achieved a superior 18,200 W, confirming its efficiency under LW shading.

(a) TCT

11	12	13	14	15	16	17	18	19
21	22	23	24	25	26	27	28	29
31	32	33	34	35	36	37	38	39
41	42	43	44	45	46	47	48	49
51	52	53	54	55	56	57	58	59
61	62	63	64	65	66	67	68	69
71	72	73	74	75	76	77	78	79
81	82	83	84	85	86	87	88	89
91	92	93	94	95	96	97	98	99

(b) BOA

11	12	13	14	15	16	17	18	19
21	22	23	24	25	26	27	28	29
31	32	33	34	35	36	37	38	39
41	42	43	44	45	46	47	48	49
51	52	53	54	55	56	57	58	59
61	62	63	64	65	66	67	68	69
71	72	73	74	75	76	77	78	79
81	82	83	84	85	86	87	88	89
91	92	93	94	95	96	97	98	99

(c) FPA

11	12	13	14	15	16	17	18	19
21	22	23	24	25	26	27	28	29
31	32	33	34	35	36	37	38	39
41	42	43	44	45	46	47	48	49
51	52	53	54	55	56	57	58	59
61	62	63	64	65	66	67	68	69
71	72	73	74	75	76	77	78	79
81	82	83	84	85	86	87	88	89
91	92	93	94	95	96	97	98	99

(d) HHO

11	12	13	14	15	16	17	18	19
21	22	23	24	25	26	27	28	29
31	32	33	34	35	36	37	38	39
41	42	43	44	45	46	47	48	49
51	52	53	54	55	56	57	58	59
61	62	63	64	65	66	67	68	69
71	72	73	74	75	76	77	78	79

900 w/m^2 600 w/m^2 500 w/m^2 400 w/m^2 200 w/m^2

Figure 6: LW shading pattern applied to PV arrays using: (a) TCT, (b) BOA, (c) FPA, (d) HHO, and (e) SO-based configurations.

International Journal of Environmental Sciences
ISSN: 2229-7359
Vol. 11 No. 23s, 2025
https://www.theaspd.com/ijes.php

	81	82	83	84	85	86	87	88	89
	91	92	93	94	95	96	97	98	99
(e)	**SO**								
	11	12	13	14	15	16	17	18	19
	21	22	23	24	25	26	27	28	29
	31	32	33	34	35	36	37	38	39
	41	42	43	44	45	46	47	48	49
	51	52	53	54	55	56	57	58	59
	61	62	63	64	65	66	67	68	69
	71	72	73	74	75	76	77	78	79
	81	82	83	84	85	86	87	88	89
	91	92	93	94	95	96	97	98	99

Row	**I(A)**	**V(v)**	**P(W)**
TCT			
R_1	6.6	6	39.6
R_2	6.6	6	39.6
R_3	6.6	6	39.6
R_4	6.6	6	39.6
R_5	6.6	6	39.6
R_6	6.6	6	39.6
R_7	6.1	9	32.9
R_8	6.1	9	32.9
R_9	6.1	9	32.9
BOA			
R_1	5.5	8	44.0
R_2	5.7	4	22.8
R_3	5.3	9	47.7
R_4	5.6	7	39.2
R_5	5.7	4	22.8
R_6	5.7	4	22.8
R_7	5.7	4	22.8
R_8	5.6	7	39.2
R_9	5.6	7	39.2
FPA			
R_1	5.6	4	22.4

R_2	6.6	2	13.2
R_3	5.0	8	40.0
R_4	5.5	5	27.5
R_5	6.6	1	13.2
R_6	5.4	6	32.4
R_7	6.2	3	18.6
R_8	4.5	9	40.5
R_9	5.0	8	40.5
HHO			
R_1	5.5	5	27.5
R_2	5.2	9	46.8
R_3	5.5	5	27.5
R_4	5.5	5	27.5
R_5	5.4	8	43.2
R_6	6.4	1	6.4
R_7	5.7	3	17.1
R_8	5.4	8	43.2
R_9	5.8	2	11.6
SO			
R_1	5.9	2	11.8
R_2	5.4	9	48.6
R_3	5.6	5	28.0
R_4	5.4	9	48.6
R_5	5.5	7	38.5
R_6	5.6	5	28.0
R_7	5.5	7	38.5
R_8	5.6	5	28.0
R_9	5.9	2	11.8

Table 4: Comparison of Global Maximum Power for TCT, BOA, FPA, HHO, and the proposed SO-based configurations under LW shading conditions.

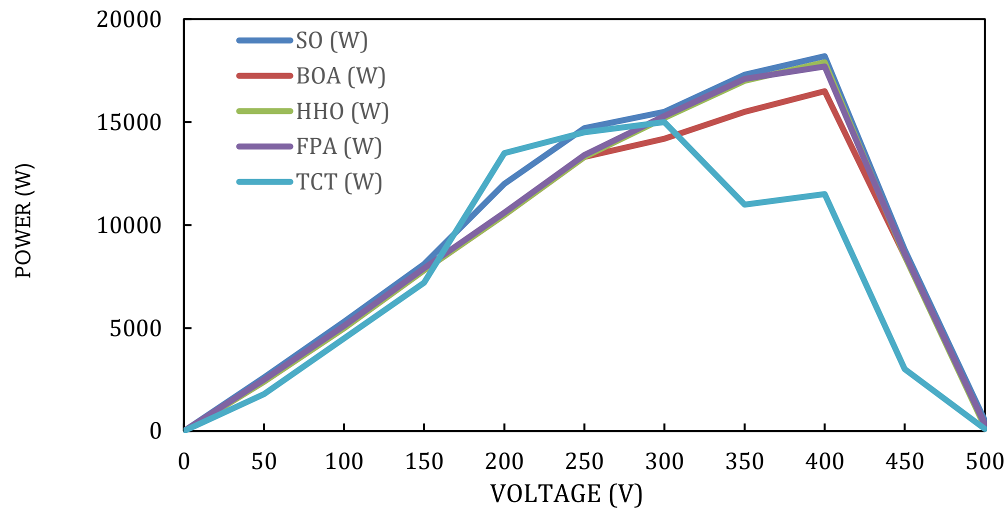

Figure 7: Comparison of voltage-power responses for various configurations under LW shadow conditions.

6.3. Case 3: Short Narrow (SN) Shading Pattern

In the SN shading case, the PV array is exposed to three irradiance levels: 900, 600, and 400 W/m². Figure 8 shows the configurations developed using the proposed SO method and other techniques. TCT, shown in Figure 8(a), yields specific row currents calculated in Equation (30), ranging from 6.1 I_m to 8.1 I_m.

$$I_{R8} = I_{R9} = 5 \times 0.9\ I_m + 4 \times 0.6\ I_m = 6.1\ I_m \quad (30a)$$

$$I_{R6} = I_{R7} = 5 \times 0.9\ I_m + 2 \times 0.6\ I_m + 2 \times 0.4\ I_m = 7.3\ I_m \quad (30b)$$

$$I_{R1} = I_{R2} = I_{R3} = I_{R4} = I_{R5} = 9 \times 0.9\ I_m = 8.1\ I_m \quad (30c)$$

Table 5 tabulate the row currents and corresponding GMP values. TCT produced the lowest peak power at 54.9 W, while HHO improved it to 58.4 W. BOA and FPA both achieved 61.2 W, and the SO method outperformed all, reaching 65.7 W representing a 19.7% gain over TCT and notable improvements over other methods. Figure 9 presents the voltage-power curves, where the SO configuration also delivers the highest GMP of 18,201 W, compared to 16,501 W for TCT, confirming its superior performance.

(a)

TCT								
11	12	13	14	15	16	17	18	19
21	22	23	24	25	26	27	28	29
31	32	33	34	35	36	37	38	39
41	42	43	44	45	46	47	48	49
51	52	53	54	55	56	57	58	59
61	62	63	64	65	66	67	68	69
71	72	73	74	75	76	77	78	79
81	82	83	84	85	86	87	88	89
91	92	93	94	95	96	97	98	99

(b)

BOA								
11	12	13	14	15	16	17	18	19
21	22	23	24	25	26	27	28	29
31	32	33	34	35	36	37	38	39
41	42	43	44	45	46	47	48	49

900 w/m^2 600 w/m^2 400 w/m^2

Figure 8: Global Maximum Power Comparison among TCT, BOA, FPA, HHO, and the proposed SO-based configurations under LW shading.

	51	52	53	54	55	56	57	58	59
	61	62	63	64	65	66	67	68	69
	71	72	73	74	75	76	77	78	79
	81	82	83	84	85	86	87	88	89
	91	92	93	94	95	96	97	98	99
(c)	**FPA**								
	11	12	13	14	15	16	17	18	19
	21	22	23	24	25	26	27	28	29
	31	32	33	34	35	36	37	38	39
	41	42	43	44	45	46	47	48	49
	51	52	53	54	55	56	57	58	59
	61	62	63	64	65	66	67	68	69
	71	72	73	74	75	76	77	78	79
	81	82	83	84	85	86	87	88	89
	91	92	93	94	95	96	97	98	99
(d)	**HHO**								
	11	12	13	14	15	16	17	18	19
	21	22	23	24	25	26	27	28	29
	31	32	33	34	35	36	37	38	39
	41	42	43	44	45	46	47	48	49
	51	52	53	54	55	56	57	58	59
	61	62	63	64	65	66	67	68	69
	71	72	73	74	75	76	77	78	79
	81	82	83	84	85	86	87	88	89
	91	92	93	94	95	96	97	98	99
(e)	**SO**								
	11	12	13	14	15	16	17	18	19
	21	22	23	24	25	26	27	28	29
	31	32	33	34	35	36	37	38	39
	41	42	43	44	45	46	47	48	49
	51	52	53	54	55	56	57	58	59
	61	62	63	64	65	66	67	68	69
	71	72	73	74	75	76	77	78	79
	81	82	83	84	85	86	87	88	89
	91	92	93	94	95	96	97	98	99

Row	**I(A)**	**V(v)**	**P(W)**
TCT			
R_1	8.1	5	40.5
R_2	8.1	5	40.5
R_3	8.1	5	40.5
R_4	8.1	5	40.5
R_5	8.1	5	40.5
R_6	7.3	7	51.1
R_7	7.3	7	51.1
R_8	6.1	9	54.9

R_9	6.1	9	54.9
BOA			
R_1	7.5	6	45.0
R_2	8.1	1	8.1
R_3	7.8	3	23.4
R_4	7.8	3	23.4
R_5	6.8	9	61.2
R_6	7.5	6	45.0
R_7	7.0	8	56.0
R_8	7.3	8	56.0
R_9	7.5	6	45.0z
FPA			
R_1	6.8	9	61.2
R_2	7.3	8	58.4
R_3	7.5	6	45.0
R_4	7.5	6	45.0
R_5	7.3	8	58.4
R_6	7.5	6	45.0
R_7	7.5	6	45.0
R_8	7.8	2	15.6
R_9	8.1	1	8.1
HHO			
R_1	7.3	8	58.4
R_2	7.3	8	58.4
R_3	7.3	8	58.4
R_4	7.5	5	37.5
R_5	8.1	1	8.1
R_6	7.5	5	37.5
R_7	7.2	5	37.5

R_8	7.5	5	37.5
R_9	7.6	2	15.2
SO			
R_1	7.5	6	45.0
R_2	7.3	9	65.7
R_3	7.5	6	45.0
R_4	7.3	9	65.7
R_5	7.6	2	15.2
R_6	7.8	1	7.8
R_7	7.5	6	45.0
R_8	7.5	6	45.0
R_9	7.3	9	65.7

Table 5 Global Maximum Power outcomes for TCT, BOA, FPA, HHO, and the proposed SO method under LW shading conditions.

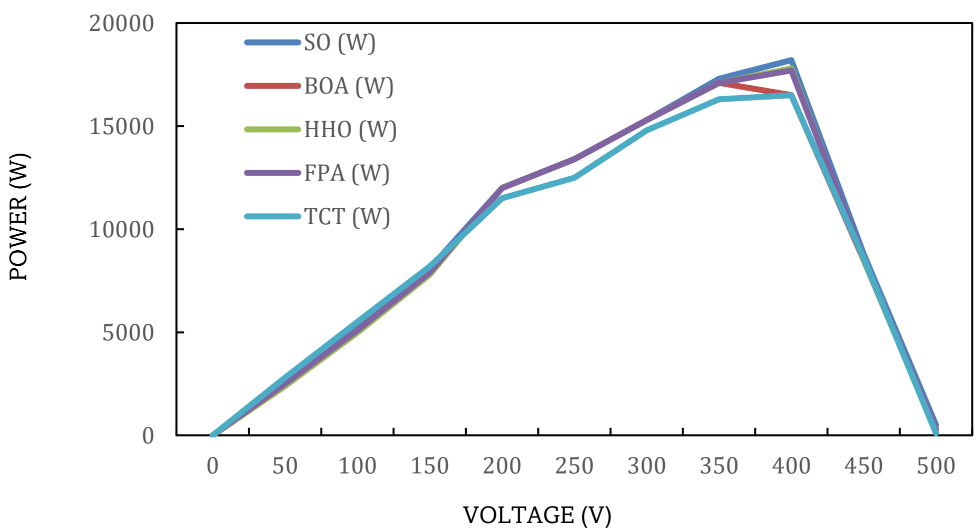

Figure 9: Voltage-power characteristics of TCT, BOA, HHO, FPA, and SO configurations under SN shading conditions.

Case 4: Long Narrow Shading Pattern

In the final shading scenario, the PV array receives four radiation levels: 900, 700, 400, and 300 W/m², mainly affecting its last three columns. Figure 10 compares the proposed method to others techniques, with TCT shown in Figure 10(a). Row currents are calculated as:

$I_{R8} = I_{R9} = 6 \times 0.9I_m + 3 \times 0.3I_m = 6.3I_m$ (31a)

$I_{R6} = I_{R7} = 6 \times 0.9I_m + 3 \times 0.4I_m = 6.6I_m$ (31b)

$IR3 = IR4 = IR5 = 7 \times 0.9Im + 2 \times 0.7Im = 7.7Im$ (31c)

$I_{R1} = I_{R2} = 9 \times 0.9I_m = 8.1I_m$ (31d)

Table 6 summarizes the results. Both TCT and FPA yielded the lowest peak output (56.7 W), while BOA and HHO improved it to 61.2 W and 62.1 W, respectively. The proposed SO method achieved the highest output of 64.0 W, marking gains of 12.9% over TCT and FPA, 4.6% over BOA, and 3.1% over HHO. Figure 11 shows voltage-power curves, with the SO method reaching the highest GMP at 18,832 W, compared to 16,501 W from the TCT configuration.

(a)

TCT								
11	12	13	14	15	16	17	18	19
21	22	23	24	25	26	27	28	29
31	32	33	34	35	36	37	38	39
41	42	43	44	45	46	47	48	49
51	52	53	54	55	56	57	58	59
61	62	63	64	65	66	67	68	69
71	72	73	74	75	76	77	78	79
81	82	83	84	85	86	87	88	89
91	92	93	94	95	96	97	98	99

(b)

BOA								
11	12	13	14	15	16	17	18	19
21	22	23	24	25	26	27	28	29
31	32	33	34	35	36	37	38	39
41	42	43	44	45	46	47	48	49
51	52	53	54	55	56	57	58	59
61	62	63	64	65	66	67	68	69
71	72	73	74	75	76	77	78	79
81	82	83	84	85	86	87	88	89
91	92	93	94	95	96	97	98	99

(c)

FPA								
11	12	13	14	15	16	17	18	19
21	22	23	24	25	26	27	28	29
31	32	33	34	35	36	37	38	39
41	42	43	44	45	46	47	48	49
51	52	53	54	55	56	57	58	59
61	62	63	64	65	66	67	68	69
71	72	73	74	75	76	77	78	79
81	82	83	84	85	86	87	88	89
91	92	93	94	95	96	97	98	99

(d)

HHO								
11	12	13	14	15	16	17	18	19
21	22	23	24	25	26	27	28	29
31	32	33	34	35	36	37	38	39
41	42	43	44	45	46	47	48	49
51	52	53	54	55	56	57	58	59
61	62	63	64	65	66	67	68	69

900 w/m^2 700 w/m^2 400 w/m^2 300 w/m^2

Figure 11: Comparative voltage-power characteristics of different PV configurations under the SN shadow pattern.

	71	72	73	74	75	76	77	78	79
	81	82	83	84	85	86	87	88	89
	91	92	93	94	95	96	97	98	99
(e)	**SO**								
	11	12	13	14	15	16	17	18	19
	21	22	23	24	25	26	27	28	29
	31	32	33	34	35	36	37	38	39
	41	42	43	44	45	46	47	48	49
	51	52	53	54	55	56	57	58	59
	61	62	63	64	65	66	67	68	69
	71	72	73	74	75	76	77	78	79
	81	82	83	84	85	86	87	88	89
	91	92	93	94	95	96	97	98	99

Row	**I(A)**	**V(v)**	**P(W)**
TCT			
R_1	8.1	2	16.2
R_2	8.1	2	16.2
R_3	7.7	5	38.5
R_4	7.7	5	38.5
R_5	7.7	5	38.5
R_6	6.6	7	46.2
R_7	6.6	7	46.2
R_8	6.3	9	56.7
R_9	6.3	9	56.7
BOA			
R_1	6.8	9	61.2
R_2	7.6	2	15.2
R_3	7.3	5	36.5
R_4	8.1	1	8.1
R_5	7.0	6	42.0
R_6	6.9	7	48.3
R_7	6.8	9	61.2
R_8	7.3	5	36.5
R_9	7.3	5	36.5
FPA			

R_1	7.4	4	29.6
R_2	7.6	3	22.8
R_3	6.8	8	54.4
R_4	7.1	6	46.2
R_5	8.1	1	8.1
R_6	6.8	8	54.4
R_7	6.3	9	56.7
R_8	7.3	5	36.5
R_9	7.7	2	15.4
HHO			
R_1	7.9	1	7.9
R_2	7.4	3	22.2
R_3	6.9	9	62.1
R_4	7.1	7	49.7
R_5	7.1	7	49.7
R_6	6.9	9	62.1
R_7	7.4	3	22.2
R_8	7.1	7	49.7
R_9	7.3	4	29.2
SO			
R_1	7.3	6	43.8
R_2	7.4	2	14.8
R_3	7.1	7	49.7
R_4	7.3	6	43.8
R_5	7.0	9	64.0
R_6	7.4	2	14.8
R_7	7.3	6	43.8
R_8	7.3	6	43.8
R_9	7.0	9	64.0

Table 6: Global maximum power comparison among TCT, BOA, FPA, HHO, and the proposed SO-based configurations under LW shading.

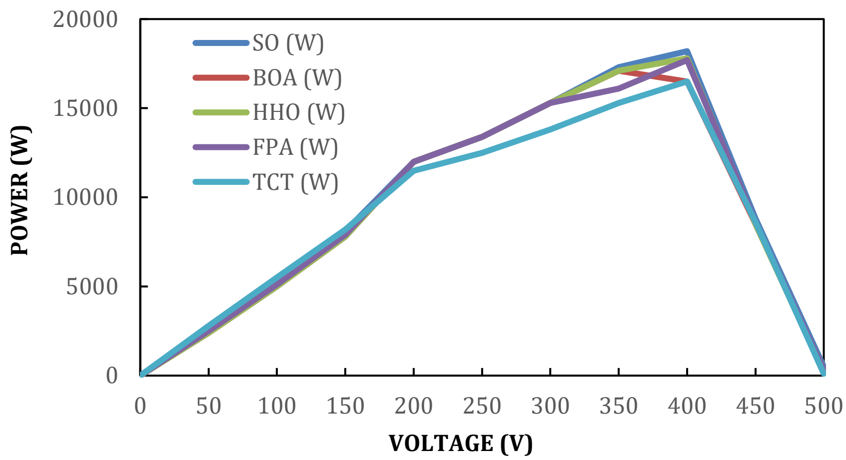

Figure 10: LW shading distribution across PV arrays as configured by: (a) TCT, (b) BOA, (c) FPA, (d) HHO, and (e) SO method.

7. ASSESSMENT CRITERIA FOR PV ARRAY PERFORMANCE

To actually evaluate the effectiveness of various PV array reconfiguration strategies, a comprehensive performance assessment is essential. This study utilizes several performance metrics to compare the proposed method based on the Snake Optimizer-based method with established techniques under partial shading conditions. The comparison includes the Total Cross Tied (TCT), Butterfly Optimization Algorithm (BOA), Flower Pollination Algorithm (FPA), and Harris Hawks Optimization (HHO) configurations. To ensure fair benchmarking, key indicators such as the Global Maximum Power (GMP), Fill Factor (FF), Mismatch Loss (ML), and overall conversion efficiency are applied. The definitions and computational methods for these indicators are outlined below:

$$\boldsymbol{FF} = \frac{\boldsymbol{Pm}}{\boldsymbol{V_{oc}} \times \boldsymbol{I_{sc}}} \quad (32)$$

a) Power Loss (PL)

PL measures the reduction in power output due to shading. It is defined as the percentage loss relative to power under uniform irradiance ($P_{uniform}$) and is calculated using (Rezazadeh et al., 2023):

$$\boldsymbol{PL} = \frac{\boldsymbol{P_{uniform}} - \boldsymbol{P_{PSc}}}{\boldsymbol{P_{uniform}}} \quad (33)$$

b) Conversion Efficiency (η)

Efficiency refers to the proportion of solar energy that is successfully converted into usable electrical power. It is calculated as (Rezazadeh et al., 2023):

$$\boldsymbol{\eta} = \frac{\boldsymbol{Pm}}{\boldsymbol{Pin}} \quad (34)$$

where $\boldsymbol{Pm}$ is the maximum power point, and $\boldsymbol{Pin}$ is the incident solar power.

Figures 12(a-d) present the graphical comparison of FF, PL, and η under four common shading patterns: Short Wide (SW), Long Wide (LW), Short Narrow (SN), and Long Narrow (LN). But in all scenarios, the Snake-O algorithm out competes TCT techniques.

International Journal of Environmental Sciences
ISSN: 2229-7359
Vol. 11 No. 23s, 2025
https://www.theaspd.com/ijes.php

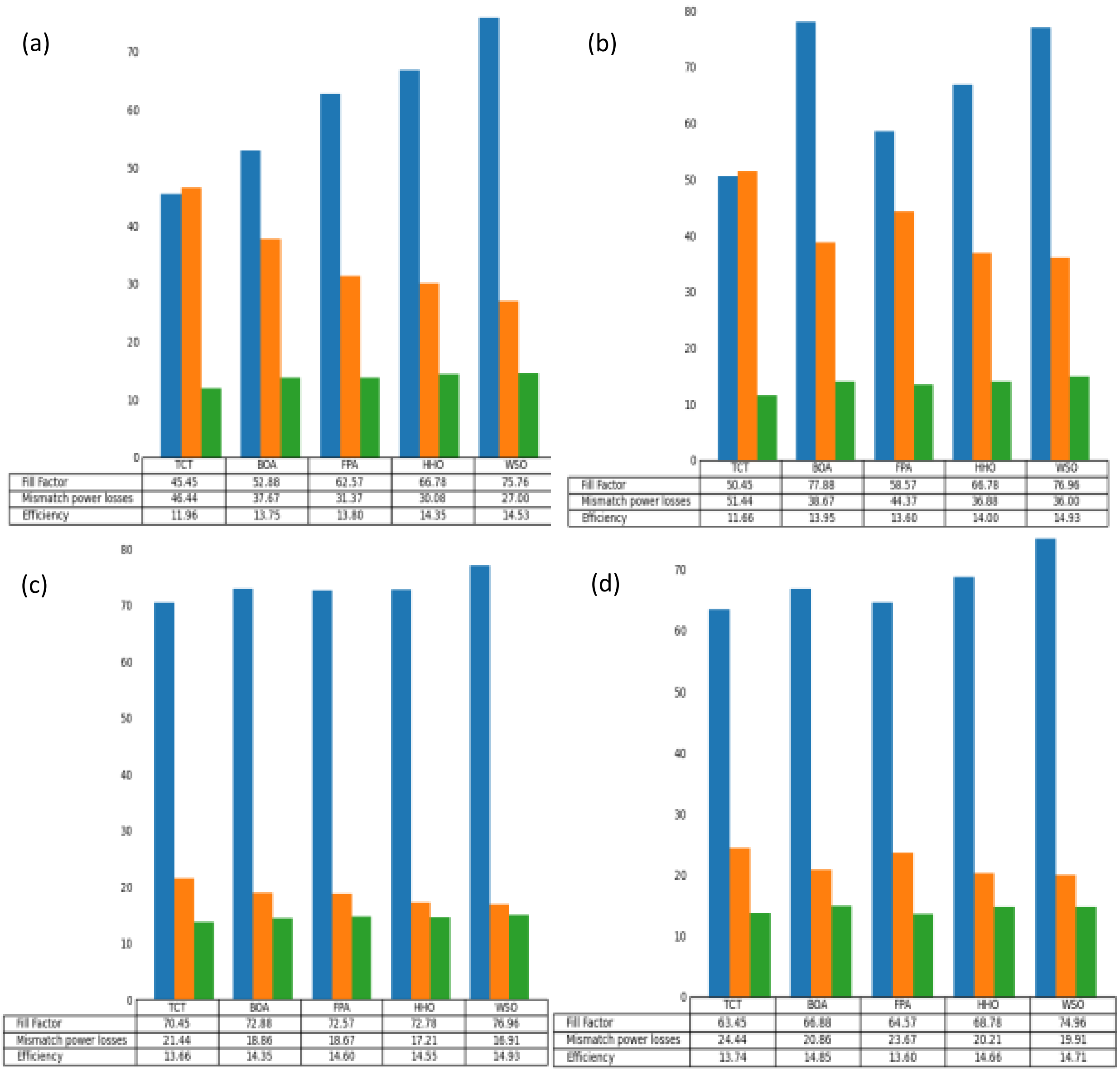

Image 12: Fill Factor (FF), Mismatch Loss (ML), and efficiency comparison for four shading scenarios a) Short, Wide (SW). b) Long Wide (L), c) Short-Narrow (SN). d) Long Narrow (LN).

8. CONCLUSION

This study applied a solution of snakes to improve the power output of photovoltaic (PV) arrays under partial shadow conditions. In comparison with traditional Total Cross Tie (TCT) methods and unlike Capital Inversion technologies (nanotubes), this operations based on SO algorithm makes ever simpler the process of shuffling modules and boosting energy production without adjustments to physical layout.

This case study employed a 9×9 PV array and subjected it to four typical shading scenarios: Short Wide (SW), Long Wide (LW), Short Narrow (SN), and Long Narrow (LN). Simulation results show that the SO algorithm outperforms traditional techniques at all test settings: TCT, Flower Pollination Algorithm (FPA), Harmony Search Optimization (HSO), and Butterfly Optimization Algorithm (BOA). Specifically, Global Maximum Power (GMP) showed a noticeable upward trend in the SW pattern: 18.51% respectively. Under the LW, the increase was, while both spots of light saw an improvement towards 10%. While SO powers from the above study have the obvious output advantage, the bio-mimicry algorithm also showed higher performance in other evaluation indices such as Fill Factor (FF), Power Loss (PL) and general conversion efficiency. By incorporating biologically-inspired strategies for both exploration and exploitation, this algorithm manages to prevent being trapped in local optima. The Snake Optimizer (SO) algorithm has the theoretical and simulation-based capabilities to deliver successful results at the real-world level. However, there are a number of practical issues that need to be faced by anyone who wishes to see this technique put into action. Computational complexity is a key matter: with larger arrays and more complex shading scenarios the computational demand of SO could increase greatly. More powerful systems may be required for real-time use Alternatively the entire algorithm must be streamlined so that it can run without pause during real-time operation. In size and performance, scalability must also come under consideration. Despite the promising results for a 9×9 PV array, what is its practical value and computational efficiency when applied to a larger real-world array? This remains an open question. Again, hardware integration responses are to be had. For a PV array to reconfigure dynamically we need advanced switching arrangements and reliable control and sensing means to do it. At least in the case of Solar Energy Systems which is currently where this technology seems most promising. The act of putting such deployments into action is sure to be complex and heavy with meaning. Economics and maintenance are also closely related, decisions will have to be made between these and practical elements if the SO approach to optimization (as it is actually applied) in modern PV systems is. The findings provide evidence that the SO algorithm is a powerful and practical optimizer for dynamically reconfiguring PV arrays. It can strike a balance between terseness in computing and reality-based employment. Deploying SO this way could lead to increased energy output in a variety of climates, making it an attractive solution for improving solar energy systems under recently changing light-political side effects. Author Contributions: Ghusoon A.Aboud: Conceptualization, Formal analysis, Investigation, Writing – original draft, Maher T. Alshamkhani; Conceptualization, Funding acquisition, Writing – review & editing, Masad Mezher Hasan; Conceptualization, Funding acquisition, Project administration, Resources, Supervision, Validation, Writing – review & editing, Ahmed Khaldoon Abdalameer.; Formal analysis, Software, Writing – review & editing. All authors have read and agreed to the published version of the manuscript.

REFERENCES

1. Aljafari, B., Satpathy, P.R., Thanikanti, S.B., 2022. Partial shading mitigation in PV arrays through dragonfly algorithm based dynamic reconfiguration. Energy 257, 124795. https://doi.org/10.1016/j.energy.2022.124795
2. Anjum, S., Mukherjee, V., 2022. A novel arithmetic sequence pattern reconfiguration technique for line loss reduction of photovoltaic array under non-uniform irradiance. Journal of Cleaner Production 331, 129822. https://doi.org/10.1016/j.jclepro.2021.129822
3. Baka, M., Manganiello, P., Soudris, D., Catthoor, F., 2019. A cost-benefit analysis for reconfigurable PV modules under shading. Solar Energy 178, 69–78. https://doi.org/10.1016/j.solener.2018.11.063
4. Cao, R., Ding, Y., Fang, X., Liang, S., Qi, F., Yang, Q., Yan, W., 2020. Photovoltaic array reconfiguration under partial shading conditions based on ant colony optimization, in: 2020 Chinese Control And Decision Conference (CCDC). Presented at the 2020 Chinese Control And Decision Conference (CCDC), pp. 703–708. https://doi.org/10.1109/CCDC49329.2020.9164084
5. Dellosa, J.T., 2016. Potential Effect and Analysis of High Residential Solar Photovoltaic (PV) Systems Penetration to an Electric Distribution Utility (DU). International Journal of Renewable Energy Development 5, 179–185. https://doi.org/10.14710/ijred.5.3.179-185
6. Fathy, A., 2018. Recent meta-heuristic grasshopper optimization algorithm for optimal reconfiguration of partially shaded PV array. Solar Energy 171, 638–651. https://doi.org/10.1016/j.solener.2018.07.014
7. Fathy, A., Yousri, D., Babu, T.S., Rezk, H., Ramadan, H.S., 2023. An enhanced reconfiguration approach for mitigating the shading effect on photovoltaic array using honey badger algorithm. Sustainable Energy Technologies and Assessments 57, 103179. https://doi.org/10.1016/j.seta.2023.103179
8. Handayani, N.A., Ariyanti, D., 2012. Potency of Solar Energy Applications in Indonesia. International Journal of Renewable Energy Development 1, 33–38. https://doi.org/10.14710/ijred.1.2.33-38
9. Hasan, M.M., Genç, G., 2022. Techno-economic analysis of solar/wind power based hydrogen production. Fuel 324, 124564. https://doi.org/10.1016/j.fuel.2022.124564
10. Hasan, M.M., González Álvarez, J.F., Qazi, I.A., Othman, M.R., 2022. Effects of membrane processed renewable biogas fuels on natural gas designed turbine's power cycle and fuel consumption. Biomass and Bioenergy 163, 106530. https://doi.org/10.1016/j.biombioe.2022.106530
11. Hasan, M.M., Murat, M.N., Kim, J., Othman, M.R., 2023. Multi-factorial central composite and complete mixing model for optimizing industrial biogas valorization. Chemical Engineering and Processing - Process Intensification 190, 109417. https://doi.org/10.1016/j.cep.2023.109417

12. Hashim, F.A., Hussien, A.G., 2022. Snake Optimizer: A novel meta-heuristic optimization algorithm. Knowledge-Based Systems 242, 108320. https://doi.org/10.1016/j.knosys.2022.108320
13. Huynh, D.C., Ho, L.D., Dunnigan, M.W., Barbalata, C., 2023. Solar Photovoltaic Array Reconfiguration for Optimizing Harvested Power Using an Advanced Artificial Bee Colony Algorithm, in: 2023 International Conference on System Science and Engineering (ICSSE). Presented at the 2023 International Conference on System Science and Engineering (ICSSE), pp. 406–411. https://doi.org/10.1109/ICSSE58758.2023.10227209
14. Jabbar, B.A., Hasan, M.M., Idroes, R., Helwani, Z., Idris, I., Othman, M.R., 2023. Effect of atmospheric distiller parameters on gasoline blend yield and research octane number of basrah crude. AIP Conference Proceedings 2785, 060002. https://doi.org/10.1063/5.0149114
15. Kumar, C.S., Rao, R.S., 2016. A Novel Global MPP Tracking of Photovoltaic System based on Whale Optimization Algorithm. International Journal of Renewable Energy Development 5, 225–232. https://doi.org/10.14710/ijred.5.3.225-232
16. Kumar, D., and Raushan, R., 2024. An innovative competence square technique for PV array reconfiguration under partial shading conditions. International Journal of Modelling and Simulation 44, 156–171. https://doi.org/10.1080/02286203.2022.2163027
17. Kumar Yadav, V., Yadav, R., Singh, R., Mishra, I., Ganvir, I., Manish, 2023. Reconfiguration of PV array through recursive addition approach for optimal power extraction under PSC. Energy Conversion and Management 292, 117412. https://doi.org/10.1016/j.enconman.2023.117412
18. Mahdavi, A., Farhadi, M., Gorji Bandpy, M., Mahmoudi, A., 2025. A Novel Non-linear Analytical Solution for Thermal Performance of a Photovoltaic Module in Vicinity of Phase-changing Materials. Renewable Energy Research and Applications 6, 105–204. https://doi.org/10.22044/rera.2024.13663.1258
19. Malathy, S., Ramaprabha, R., 2018. Reconfiguration strategies to extract maximum power from photovoltaic array under partially shaded conditions. Renewable and Sustainable Energy Reviews 81, 2922–2934. https://doi.org/10.1016/j.rser.2017.06.100
20. Mao, M., Cui, L., Zhang, Q., Guo, K., Zhou, L., Huang, H., 2020. Classification and summarization of solar photovoltaic MPPT techniques: A review based on traditional and intelligent control strategies. Energy Reports 6, 1312–1327. https://doi.org/10.1016/j.egyr.2020.05.013
21. Matha, G.M., Rao, L., 2020. Genetic Algorithm Based PV Array Reconfiguration for Improving Power Output under Partial Shadings. International Journal of Renewable Energy Research (IJRER) 10, 803–812.
22. Mirjalili, S., Saremi, S., Mirjalili, S.M., Coelho, L. dos S., 2016. Multi-objective grey wolf optimizer: A novel algorithm for multi-criterion optimization. Expert Systems with Applications 47, 106–119. https://doi.org/10.1016/j.eswa.2015.10.039
23. Mohammad, A.T., Hussen, H.M., Akeiber, H.J., 2023. Prediction of the output power of photovoltaic module using artificial neural networks model with optimizing the neurons number. International Journal of Renewable Energy Development 12, 478–487. https://doi.org/10.14710/ijred.2023.49972
24. Oko, C.O.C., Diemuodeke, E.O., Omunakwe, E.O., Nnamdi, E., 2012. Design and Economic Analysis of a Photovoltaic System: A Case Study. International Journal of Renewable Energy Development 1, 65–73. https://doi.org/10.14710/ijred.1.3.65-73
25. AlShourbaji, I., Helian, N., Sun, Y. et al. An efficient churn prediction model using gradient boosting machine and metaheuristic optimization. Sci Rep 13, 14441 (2023). https://doi.org/10.1038/s41598-023-41093-6
26. Nimma, D., Aarif, M., Pokhriyal, S., Murugan, R., Rao, V. S., & Bala, B. K. (2024, December). Artificial Intelligence Strategies for Optimizing Native Advertising with Deep Learning. In 2024 International Conference on Artificial Intelligence and Quantum Computation-Based Sensor Application (ICAIQSA) (pp. 1-6). IEEE.
27. Al-Shourbaji, I., Alhameed, M., Katrawi, A., Jeribi, F., Alim, S. (2022). A Comparative Study for Predicting Burned Areas of a Forest Fire Using Soft Computing Techniques. In: Kumar, A., Senatore, S., Gunjan, V.K. (eds) ICDSMLA 2020. Lecture Notes in Electrical Engineering, vol 783. Springer, Singapore. https://doi.org/10.1007/978-981-16-3690-5_22
28. Dash, C., Ansari, M. S. A., Kaur, C., El-Ebiary, Y. A. B., Algani, Y. M. A., & Bala, B. K. (2025, March). Cloud computing visualization for resources allocation in distribution systems. In AIP Conference Proceedings (Vol. 3137, No. 1). AIP Publishing.
29. Jameel, Mohammed & Abouhawwash, Mohamed. (2023). A new proximity metric based on optimality conditions for single and multi-objective optimization: Method and validation. Expert Systems with Applications. 241. 122677. 10.1016/j.eswa.2023.122677.
30. Kumar, A. P., Fatma, G., Sarwar, S., & Punithaasree, K. S. (2025, January). Adaptive Learning Systems for English Language Education based on AI-Driven System. In 2025 International Conference on Intelligent Systems and Computational Networks (ICISCN) (pp. 1-5). IEEE.

31. Wang, Shuang & Hussien, Ganna & Kumar, Sumit & Alshourbaji, Ibrahim & A.Hashim, Fatma. (2023). A modified Smell Agent Optimization for Global Optimization and Industrial Engineering Design Problems. Korean Journal of Computational Design and Engineering. 10. 10.1093/jcde/qwad062.
32. Elkady, G., Sayed, A., Priya, S., Nagarjuna, B., Haralayya, B., & Aarif, M. (2024). An Empirical Investigation into the Role of Industry 4.0 Tools in Realizing Sustainable Development Goals with Reference to Fast Moving Consumer Foods Industry. In Advanced Technologies for Realizing Sustainable Development Goals: 5G, AI, Big Data, Blockchain, and Industry 4.0 Application (pp. 193-203). Bentham Science Publishers.
33. Al-Shourbaji, I., & Duraibi, S. (2023). IWQP4Net: An Efficient Convolution Neural Network for Irrigation Water Quality Prediction. Water, 15(9), 1657. https://doi.org/10.3390/w15091657
34. Kaur, C., Al Ansari, M. S., Rana, N., Haralayya, B., Rajkumari, Y., & Gayathri, K. C. (2024). A Study Analyzing the Major Determinants of Implementing Internet of Things (IoT) Tools in Delivering Better Healthcare Services Using Regression Analysis. In Advanced Technologies for Realizing Sustainable Development Goals: 5G, AI, Big Data, Blockchain, and Industry 4.0 Application (pp. 270-282). Bentham Science Publishers.
35. Alshourbaji, Ibrahim & Jabbari, Abdoh & Rizwan, Shaik & Mehanawi, Mostafa & Mansur, Phiros & Abdalraheem, Mohammed. (2025). An Improved Ant Colony Optimization to Uncover Customer Characteristics for Churn Prediction. Computational Journal of Mathematical and Statistical Sciences. 4. 17-40. 10.21608/cjmss.2024.298501.1059.
36. Alijoyo, F. A., Prabha, B., Aarif, M., Fatma, G., & Rao, V. S. (2024, July). Blockchain-Based Secure Data Sharing Algorithms for Cognitive Decision Management. In 2024 International Conference on Electrical, Computer and Energy Technologies (ICECET (pp. 1-6). IEEE.
37. Abouhawwash, Mohamed & Jameel, Mohammed & Askar, S.S.. (2023). Multi-Criteria Decision Making Model for Analysis Hydrogen Production for Economic Feasibility and Sustainable Energy. Multicriteria Algorithms with Applications. 1. 31-41. 10.61356/j.mawa.2023.16161.
38. Elkady, G., Sayed, A., Mukherjee, R., Lavanya, D., Banerjee, D., & Aarif, M. (2024). A Critical Investigation into the Impact of Big Data in the Food Supply Chain for Realizing Sustainable Development Goals in Emerging Economies. In Advanced Technologies for Realizing Sustainable Development Goals: 5G, AI, Big Data, Blockchain, and Industry 4.0 Application (pp. 204-214). Bentham Science Publishers.
39. Jameel, Mohammed & Abouhawwash, Mohamed. (2023). A Reference Point-Based Evolutionary Algorithm Solves Multi and Many-Objective Optimization Problems: Method and Validation. Computational Intelligence and Neuroscience. 2023. 4387053. 10.1155/2023/4387053.
40. Praveena, K., Misba, M., Kaur, C., Al Ansari, M. S., Vuyyuru, V. A., & Muthuperumal, S. (2024, July). Hybrid MLP-GRU Federated Learning Framework for Industrial Predictive Maintenance. In 2024 Third International Conference on Electrical, Electronics, Information and Communication Technologies (ICEEICT) (pp. 1-8). IEEE.
41. Alshourbaji, Ibrahim & Kachare, Pramod & Fadlelseed, Sajid & Jabbari, Abdoh & Hussien, Ganna & AL Saqqar, Faisal & Abualigah, Laith & Alameen, Abdalla. (2023). Artificial Ecosystem-Based Optimization with Dwarf Mongoose Optimization for Feature Selection and Global Optimization Problems. International Journal of Computational Intelligence Systems. 16. 10.1007/s44196-023-00279-6.
42. Orosoo, M., Rajkumari, Y., Ramesh, K., Fatma, G., Nagabhaskar, M., Gopi, A., & Rengarajan, M. (2024). Enhancing English Learning Environments Through Real-Time Emotion Detection and Sentiment Analysis. International Journal of Advanced Computer Science & Applications, 15(7).
43. D. V. Puri et al., "LEADNet: Detection of Alzheimer's Disease Using Spatiotemporal EEG Analysis and Low-Complexity CNN," in IEEE Access, vol. 12, pp. 113888-113897, 2024, doi: 10.1109/ACCESS.2024.3435768.
44. Tripathi, M. A., Goswami, I., Haralayya, B., Roja, M. P., Aarif, M., & Kumar, D. (2024). The Role of Big Data Analytics as a Critical Roadmap for Realizing Green Innovation and Competitive Edge and Ecological Performance for Realizing Sustainable Goals. In Advanced Technologies for Realizing Sustainable Development Goals: 5G, AI, Big Data, Blockchain, and Industry 4.0 Application (pp. 260-269). Bentham Science Publishers.
45. Palpandian, M., Winston, D.P., Kumar, B.P., Kumar, C.S., Babu, T.S., Alhelou, H.H., 2021. A New Ken-Ken Puzzle Pattern Based Reconfiguration Technique for Maximum Power Extraction in Partial Shaded Solar PV Array. IEEE Access 9, 65824–65837. https://doi.org/10.1109/ACCESS.2021.3076608
46. Pandey, P.K., Sandhu, K.S., 2014. Multi diode modelling of PV cell, in: 2014 IEEE 6th India International Conference on Power Electronics (IICPE). Presented at the 2014 IEEE 6th India International Conference on Power Electronics (IICPE), pp. 1–4. https://doi.org/10.1109/IICPE.2014.7115793
47. Petrychenko, O., Levinskyi, M., Goolak, S., Lukoševičius, V., 2025. Prospects of Solar Energy in the Context of Greening Maritime Transport. Sustainability 17, 2141. https://doi.org/10.3390/su17052141
48. Pillai, D.S., Rajasekar, N., Ram, J.P., Chinnaiyan, V.K., 2018. Design and testing of two phase array reconfiguration procedure for maximizing power in solar PV systems under partial shade conditions (PSC). Energy Conversion and Management 178, 92–110. https://doi.org/10.1016/j.enconman.2018.10.020

49. Rezazadeh, S., Moradzadeh, A., Pourhossein, K., Mohammadi-Ivatloo, B., García Márquez, F.P., 2023. Photovoltaic array reconfiguration under partial shading conditions for maximum power extraction via knight's tour technique. J Ambient Intell Human Comput 14, 11545–11567. https://doi.org/10.1007/s12652-022-03723-1
50. Rezk, H., Fathy, A., Aly, M., 2021. A robust photovoltaic array reconfiguration strategy based on coyote optimization algorithm for enhancing the extracted power under partial shadow condition. Energy Reports 7, 109–124. https://doi.org/10.1016/j.egyr.2020.11.035
51. Romli, M.I.F., Rajkumar, R.K., Wan, W.Y., Wai, C.L., Arelhi, R., Isa, D., 2016. The Effectiveness of New Solar Photovoltaic System with Supercapacitor for Rural Areas. International Journal of Renewable Energy Development 5, 249–257. https://doi.org/10.14710/ijred.5.3.249-257
52. Rumbayan, M., Kindangen, J., Sambul, A., Sompie, S., Cross, J., 2025. Solar energy implementation in rural communities and its contributions to SDGs: A systematic literature review. Unconventional Resources 6, 100180. https://doi.org/10.1016/j.uncres.2025.100180
53. Sai Krishna, G., Moger, T., 2018. SuDoKu and Optimal SuDoKu Reconfiguration for TCT PV array Under Non-Uniform Irradiance Condition, in: 2018 IEEE 8th Power India International Conference (PIICON). Presented at the 2018 IEEE 8th Power India International Conference (PIICON), pp. 1–6. https://doi.org/10.1109/POWERI.2018.8704458
54. Talukdar, K., 2017. Modeling and Analysis of Solar Photovoltaic Assisted Electrolyzer-Polymer Electrolyte Membrane Fuel Cell For Running a Hospital in Remote Area in Kolkata, India. International Journal of Renewable Energy Development 6, 181–191. https://doi.org/10.14710/ijred.6.2.181-191
55. Venkateswari, R., Rajasekar, N., 2021. Modified Lo Shu Technique for Power Enhancement of a Partially Shaded PV array, in: 2021 Innovations in Power and Advanced Computing Technologies (i-PACT). Presented at the 2021 Innovations in Power and Advanced Computing Technologies (i-PACT), pp. 1–7. https://doi.org/10.1109/i-PACT52855.2021.9696737
56. Yang, B., Ye, Haoyin, Wang, J., Li, J., Wu, S., Li, Y., Shu, H., Ren, Y., Ye, Hua, 2021. PV arrays reconfiguration for partial shading mitigation: Recent advances, challenges and perspectives. Energy Conversion and Management 247, 114738. https://doi.org/10.1016/j.enconman.2021.114738
57. Yang, Y., Chen, H., Heidari, A.A., Gandomi, A.H., 2021. Hunger games search: Visions, conception, implementation, deep analysis, perspectives, and towards performance shifts. Expert Systems with Applications 177, 114864. https://doi.org/10.1016/j.eswa.2021.114864
58. Yousri, D., Allam, D., Eteiba, Magdy.B., 2020a. Optimal photovoltaic array reconfiguration for alleviating the partial shading influence based on a modified harris hawks optimizer. Energy Conversion and Management 206, 112470. https://doi.org/10.1016/j.enconman.2020.112470
59. Yousri, D., Allam, D., Eteiba, M.B., Suganthan, P.N., 2019a. Static and dynamic photovoltaic models' parameters identification using Chaotic Heterogeneous Comprehensive Learning Particle Swarm Optimizer variants. Energy Conversion and Management 182, 546–563. https://doi.org/10.1016/j.enconman.2018.12.022
60. Yousri, D., Babu, T.S., Allam, D., Ramachandaramurthy, V.K., Beshr, E., Eteiba, M.B., 2019b. Fractional Chaos Maps with Flower Pollination Algorithm for Partial Shading Mitigation of Photovoltaic Systems. Energies 12, 3548. https://doi.org/10.3390/en12183548
61. Yousri, D., Thanikanti, S.B., Balasubramanian, K., Osama, A., Fathy, A., 2020b. Multi-Objective Grey Wolf Optimizer for Optimal Design of Switching Matrix for Shaded PV array Dynamic Reconfiguration. IEEE Access 8, 159931–159946. https://doi.org/10.1109/ACCESS.2020.3018722